# Partially fluorinated alumina with enhanced stability: Application to catalysis under aggressive conditions

Jean-luc Blin, Julien Dieu, Benedicte Lebeau, Laure Michelin, Séverinne Rigolet, Sylvette Brunet

# Partially Fluorinated Alumina With Enhanced Stability: Application To Catalysis Under Aggressive Conditions

Jean-Luc Blin[a*], Julien Dieu[b], Benedicte Lebeau[c,d], Laure Michelin[c,d], Séverinne Rigolet[c,d], Sylvette Brunet[1]

[a]: Université de Lorraine, CNRS, L2CM, F-54000 Nancy, France
[b] : Université de Poitiers /CNRS, IC2MP, UMR 7285, 86073 Poitiers Cedex 9 France.
[c] : Université de Haute Alsace (UHA), CNRS, IS2M UMR 7361, F-68100 Mulhouse, France
[d] : Université de Strasbourg, F-67000 Strasbourg, France

**Corresponding authors**

Pr. Jean-Luc Blin
Université de Lorraine
L2CM UMR CNRS 7053
Faculté des Sciences et Technologies
BP 70239
F-54506 Vandoeuvre-lès-Nancy cedex, France
Tel. +33 3 83 68 43 70
E-mail: Jean-Luc.Blin@univ-lorraine.fr

**Table of Contents**

Partially fluorinated alumina synthesized from an evaporation-induced self-assembly route using liquid crystals templates preserves its textural and acidic properties after being exposed under HF gas

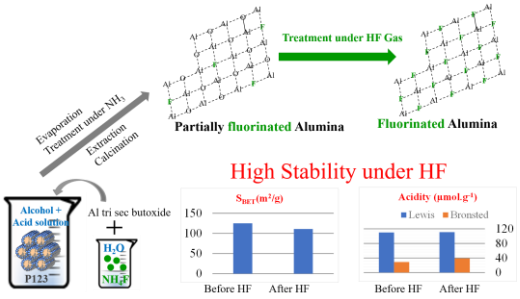

**Abstract**
Here, we report the design of new aluminum hydroxyfluoride, mainly composed of amorphous phase, with enhanced stability under HF gas in term of textural properties, especially the specific surface area and the acidity. The material has been synthesized through an EISA (evaporation-induced self-assembly) route using liquid crystals as templates. Thanks to this stability, the catalyst designed by the dispersion of the active phase on this support shows a higher accessibility and the activity of the active sites than the ones obtained by other methods

**Keywords**: Alumina, Fluoridation, Heterogeneous catalysis, Hydrogen fluoride

## 1. Introduction

Fluorinated molecules are used in the preparation of many much more sophisticated compounds with applications going from therapeutic to lithium ion batteries [1]. However, very few fluorinated organic compounds exist naturally, it is therefore necessary to develop appropriate synthesis methods. In terms of saving fluorine atoms, hydrogen fluoride (HF) is the best candidate because it represents 95% by weight of the reagent. Catalysed fluorination in the presence of HF as the fluorinating agent in the gas phase is widely carried out on an industrial scale, essentially for non-functionalized aliphatic fluorinated molecules prepared from chlorinated molecules by Cl/F exchange. In contrast, this Cl/F exchange strategy is neither applicable to functionalized aliphatic fluorinated compounds (due to the sensitivity of most organic functions towards HF), nor to fluoroaromatics, which are essentially produced by two liquid phase reactions: the Balz-Schiemann reaction (fluorodediazotation of anilines) and the HALEX reaction (HALogen EXchange) [2, 3]. These reactions generate large volumes of non-recoverable saline effluents (NaF, borates, KCl,...), organic solvents and involve toxic reagents (anilines). In addition, they are poorly selective and precursor reactivity can be limited. Clearly, new fluorination methods are needed, ideally more efficient, selective and environmentally sustainable. Such an alternative approach, already successfully used for non-functionalized aliphatic fluorinated molecules, is the one-step fluorination of chlorinated aromatic molecules via a gas phase process-based Cl/F exchange under HF involving a catalyst.

This aromatic nucleophilic substitution reaction presents many advantages, as the chloroaromatic molecules are industrially available and generally less toxic than the corresponding anilines. Additionally, no solvent is required and HCl is the only by-product which moreover is recoverable. The rare examples of these reactions described in the patent literature operate at high temperatures (400-500°C) in the presence of catalysts based on different alkali metals (Li, Na, K, Rb, Cs) or alkaline earth metals (Be, Mg, Ca, Sr, Ba) supported over activated carbon, and systematically lead to limited conversions and poor selectivity (for example, conversion of 3-chloro-2-fluoro-5-(trifluoromethyl)pyridine is only around 30% at 500°C, with a modest selectivity of 45% [4]. Better catalyst choice was recently demonstrated by S Brunet [5,6] for the fluorination of 2-chloropyridine as model molecule. Using different inorganic metal fluoride nanoparticles as efficient catalysts ($MgF_2$, $CaF_2$, $ZnF_2$, $LaF_3$, $BaF_2$ or $Ba_{1-x}La_xF_{2+x}$) [5,6], 2-fluoropyridine was obtained with 100% selectivity, at only 350°C. The best activity observed with $MgF_2$, $BaF_2$ and mixed (Ba, La) fluorides can be explained by the weak strength of Lewis acidity of the active sites preventing nitrogen-pyridine poisoning. These nanocatalysts are prepared by calcination at 400°C of trifluoroacetate (TFA) precursors leading to a notable surface area no more of 50 $m^2/g$. While the selectivity of this reaction is optimal, the activity could be enhanced by increasing the catalyst surface area and consequently the number of active sites (coordinately unsaturated metal cations), a key parameter to improve the catalytic performances. However, under the harsh conditions of anhydrous HF gas at 350°C, the nanofluoride catalysts undergo a sintering process leading to a drastic loss of the initially promising surface areas [7].

One way to overcome this drawback and thus to increase the catalytic activity, is to disperse the $MgF_2$ active phase on a porous support with high specific surface area. Indeed, in this case the active $MgF_2$ phase is obtained after wet-impregnation of the support with a magnesium precursor such as magnesium carbonate and a calcination is then carried out to decompose the precursor into MgO and $CO_2$ [8]. Finally, during the catalyst activation step under HF gas, MgO leads to the formation of $MgF_2$. When oxides such as pure alumina are used as support, during the activation step under HF gas, their fluorination also occurs, which results in a drastic drop in the specific surface area and in a modification of their catalytic properties. Kemnitz et al. by a non-aqueous route succeeded in synthesizing amorphous $AlF_3$ with a specific surface area around 200 $m^2\ g^{-1}$. However, these materials are sensitive to the temperature and the calcination

atmosphere, which results in a strong decrease of the specific surface area [9]. Therefore, $AlF_3$ prepared by this way are not good candidates to be used as support for the transformation of 2-chloropyridine under HF gas. Moreover, their behavior under HF flow is not reported in the literature. Thanks to its properties in particular the acidic ones [10], alumina serves as support for many industrial catalysts due to its ability to disperse the supported phase as well as for its moderate price [11]. The good dispersion of the active phase is associated with the presence of acid/base sites on its surface (hydroxyls). To modulate its acidic properties the introduction of fluorine, is often carried out [12]. Indeed, fluorine, which is more electronegative than oxygen, makes it possible to improve the Lewis acid character of aluminum sites. It also allows the introduction of Brønsted acid sites.
Here, we have prepared partially fluorinated alumina (aluminum hydroxyfluoride named F-$Al_2O_3$) with high stability under HF operating conditions and we have investigated their ability to be used as support for the transformation of using 2-chloropyridine in the presence of HF gas.

## 2. Experimental

### 2.1. Materials preparation.

***Partially fluorinated alumina synthesis*** (F-$Al_2O_3$)***:*** The synthesis was realized by using a procedure for mesostructured amorphous alumina [13] based on an EISA (evaporation-induced self-assembly) route using liquid crystals as templates in presence of fluorine. In a typical synthesis: 3g of P123 are dissolved under stirring at room temperature in 20 g of ethanol in the presence of citric acid (0.5 g). Then 1.5g of hydrochloric acid solution and 4g of aluminum tri sec butoxide are added. After stirring water (2g) in which ammonium fluoride (0.45g) has been previously dissolved are incorporated. The mixture is then directly evaporated under vacuum (55°C, 25mbar) to remove the solvent. Samples are dried in an oven at 40°C. Then they were placed under an atmosphere of $NH_3$ (≈ 0.5 atm) for 12 h. The amorphous fluorinated alumina is obtained after Soxhlet extraction using ethanol as solvent and calcination at 500°C under air in a muffle furnace. The samples were heated to 150°C, at a rate of 1 °C / min and kept at this temperature during one hour. Afterwards, the same program was applied to reach the final temperature. They were kept at 500°C during 2 hours and cooled down. It is labelled as F-$Al_2O_3$.
***Catalysts preparation:*** The catalysts were prepared by dry impregnation of F-$Al_2O_3$ with a solution of magnesium. The concentration of the solution is adapted to deposit 2 wt.% of Mg. After drying overnight in an oven at 110°C, the catalyst is calcined for 4 hours at 500°C under nitrogen (100 $mL.min^{-1}$).

### 2.2. Characterization.

SAXS experiments were performed on a SAXSess $mc^2$ instrument (Anton Paar), using a line collimation system. This instrument is attached to a ID 3003 laboratory X-Ray generator (General Electric) equipped with a sealed X-Ray tube (PANalytical, λ Cu, Kα = 0.1542 nm) operating at 40 kV and 50 mA. A multilayer mirror and a block collimator provide a monochromatic primary beam. A translucent beam stop allows the measurement of an attenuated primary beam at q=0. Materials were put between two sheets of Kapton® placed in a powder cell before being introduced inside the evacuated chamber. All data were corrected for the background scattering from the Kapton® and for slit-smearing effects by a desmearing procedure from SAXSQuant software using the Lake method. Powder X-ray diffraction patterns were recorded using a PANalytical X'Pert PRO diffractometer equipped with a Cu X-ray tube (λCu(Kα) = 0.1542 nm) operating at 45 kV and 40 mA and a X'Celerator detector. Fixed divergence slit (1/16°), mask (10 mm) and antiscatter slit (1/8°) were used at primary beam for the current analysis.

Transmission Electron Microscopy (TEM) observations were performed using a Jeol ARM-200F microscope working at 200kV.
$N_2$ adsorption-desorption isotherms were determined on a Micromeritics TRISTAR 3000 sorptometer at –196 °C. Prior analyses, samples were outgassed at 25°C under vacuum (0.13 bar) for 16 hours. The specific surface area was obtained by using the BET model whereas the pore diameter and the pore size distribution were determined by the BJH (Barret, Joyner, Halenda) method applied to the adsorption branch.
$^{27}Al$ MAS NMR and $^{19}F$ NMR spectra have been recorded at room temperature on a Bruker AVANCE NEO 400WB spectrometer (B0=9,4T) operating at 104.23 and 376.48 MHz respectively. Samples were packed in a 2.5 mm diameter cylindrical zirconia rotor fitted with Vespel end caps and spun at a spinning frequency of 30 kHz. $^{27}Al$ MAS NMR experiments were collected with a $\pi/12$-pulse duration of 0.33 µs and a recycle delay of 1 s. The chemical shifts were referenced to external $[Al(H_2O)_6]^{3+}$ in $AlCl_3$ aqueous solution. $^{19}F$ MAS NMR spectra have been performed with $\pi/2$-pulse duration of 2.5 µs and a recycle delay of 10 s. The chemical shifts were referred to $CFCl_3$. The central transitions are simulated by simple Gauss/Lorentz functions with the software dmfit2020 [14].
The F content in F-$Al_2O_3$ calcined at 500°C was determined using X-ray fluorescence spectrometry (XRF) performed on a Zetium XRF spectrometer (PANalytical).
The measurement of the acidity by adsorption of pyridine followed by FTIR spectroscopy was carried out with a ThermoNicolet NEXUS 5700 spectrometer at a resolution of 2 cm-1 and collected 128 scans per spectrum. Catalyst samples were pressed into thin pellets (10-60 mg) with diameter of 16 mm under a pressure of 1-2 $t.cm^{-2}$ and activated in situ during one night under nitrogen at 380°C. After cooling down the samples until room temperature, a background spectrum was collected. The quantity of Lewis and Brønsted acid sites was determined from the area of the band at 1445-1450 $cm^{-1}$ for the Lewis acidity and at 1540 $cm^{-1}$ for the Brønsted acidity. All spectra were normalized to an equivalent sample mass (20 mg) to compare them against each other.

### 2.3. Transformation of 2-chloropyridine.

Transformation of 2-chloropyridine is studied at 350°C, under atmospheric pressure, in the presence of a large excess of HF (HF/$N_2$/2-chloropyridine molar ratio = 6/1.7/1) during 4h30. For a better precision in the activity measurements, the contact time (defined as the ratio between the mass of the catalyst and the flow of the feed) was adapted to keep also the overall conversion of 2-chloropyridine nearly constant lower than 20 mol%. The catalyst is diluted in graphite, inert under the conditions used, in order to be in a differential regime.
The organic phase is analyzed by gas chromatography (GC, Scion 436-GC (Bruker)), equipped with a flame ionization detector (FID). Effective separation of the main products is obtained by a BP1 capillary column (SGE), whose characteristics are as follows: length 25 m, internal diameter 0.32 mm and phase thickness 5 µm, with a temperature program from 100 to 180°C (5°C/min). The activity measurements of the different samples for the transformation of 2-chloropyridine were carried out in an experimental set up located in a secure ventilated enclosure and located in a room dedicated to the use of this gas to protect the experimenters. An HF detector allows to prevent any danger of HF leaks both in the enclosure containing the experimental set up and in the room.

## 3. Results and discussion:

### 3.1. Structural and textural properties of F-$Al_2O_3$.

Contrary to what it is observed in the absence of fluorine, even before the treatment under HF, no line is detected on the SAXS pattern (Fig. 1). The obtained fluorinated alumina adopts a complete random mesopores arrangement. This can be due the catalytic effect of $F^-$ on the

condensation reaction of the aluminum alkoxide. Indeed, the reactivity of aluminum tri sec butoxide can be controlled by preparing the materials in an alcoholic media under strong acidic conditions [13] but when water, which contains $NH_4F$, previously dissolved, is added the uncontrolled fast precipitation of the precursor occurs.

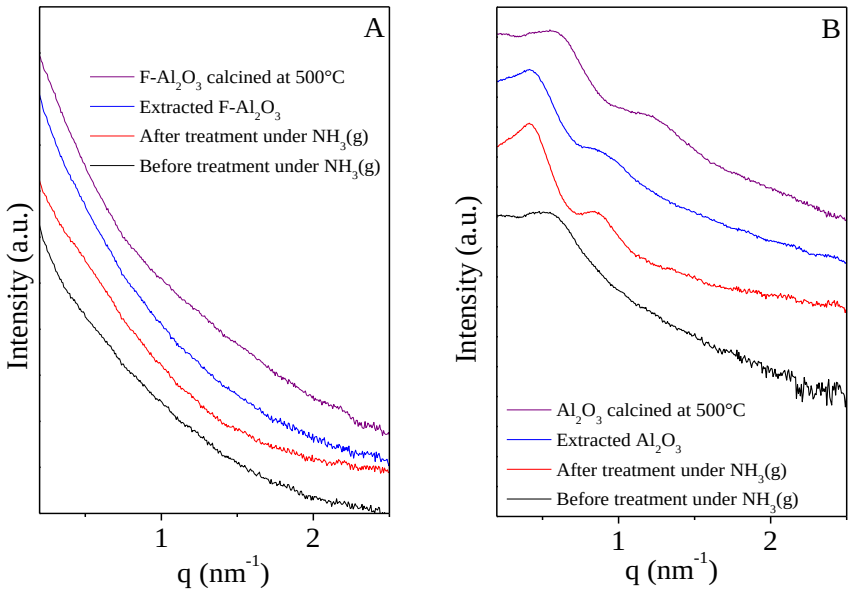


**Figure 1:** SAXS patterns of the mesoporous alumina prepared in the presence (A) and without (B) fluorine.

After extraction by ethanol Soxhlet during 8 hours a type IV isotherm with condensation step at high relative p/p° with H1 type hysteresis is obtained by nitrogen adsorption-desorption. Its shape doesn't change after calcination at 500°C or after the treatment under HF gas of the calcined materials (Fig. 2). However, the adsorbed $N_2$ volume drops from 600 to around 300 $cm^3$/g-STP after the treatment under HF.

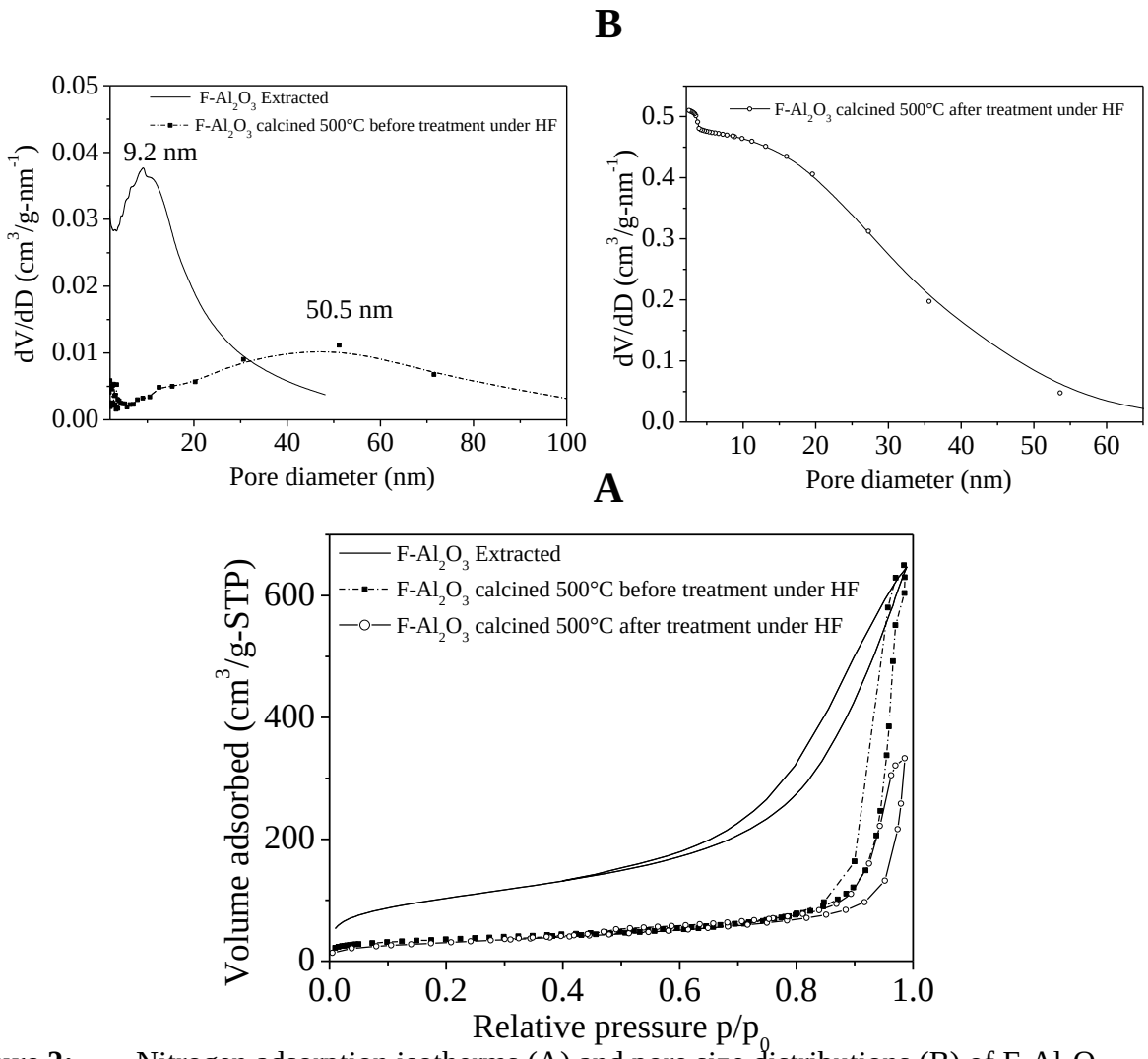


**Figure 2:** Nitrogen adsorption isotherms (A) and pore size distributions (B) of F-$Al_2O_3$.

After calcination at 500°C, the specific surface area and the pore volume decrease from 373 to 125 m²/g and from 0.83 to 0.54 $cm^3/g$, respectively (Table 1). These variations reflect the contraction of the pores network, as reflected by the values of the average mean pore diameter (Table 1). But it is interesting to note that considering the error on the measurement, about 5%, their value remains in the same range of order after the treatment under HF gas (Table 1).

**Table 1**: Specific surface area ($S_{BET}$), BJH cumulative pore volume and BJH average pore diameter of F-$Al_2O_3$ after extraction, calcination at 500°C and calcination at 500°C follow by treatment under HF.

| | F-$Al_2O_3$ Extracted | F-$Al_2O_3$ calcined 500°C before treatment under HF | F-$Al_2O_3$ calcined 500°C after treatment under HF |
|---|---|---|---|
| $S_{BET}$ (m²/g) | 373 | 125 | 111 |
| $V_P$ ($cm^3/g$) | 0.83 | 0.54 | 0.51 |
| Average pore diameter (nm) | 9.6 | 24.7 | 20.6 |

Contrary to the bulk $MgF_2$ or the commercial $AlF_3$ (Table 2), which show a strong decrease of the specific surface area around 86 and 40% after treatment under HF gas, respectively, the F-$Al_2O_3$ material exhibits a higher stability under the strong aggressive conditions. To the best of our knowledge, it is the first time that a highly stable material under these drastic conditions is obtained.

**Table 2**:. Specific surface area ($m^2.g^{-1}$) before and after treatment under HF gas

| | $MgF_2$[1] | $AlF_3$[2] | F-$Al_2O_3$ |
|---|---|---|---|
| Before treatment | 327 | 62 | 125 |
| After treatment | 45 | 37 | 111 |

[1]: prepared by hydro solvothermal method assisted by microwave heating using magnesium carbonate as precursor; [2] : commercial support

The mesoporous F-$Al_2O_3$ support before treatment under HF has been observed by TEM. A homogeneous morphology similar to bicontinous system with solid phase delimiting meso-/macropores was observed (Fig. 3). The pore sizes are quite regular and correspond to those determined from $N_2$ adsorption/desorption isotherms.

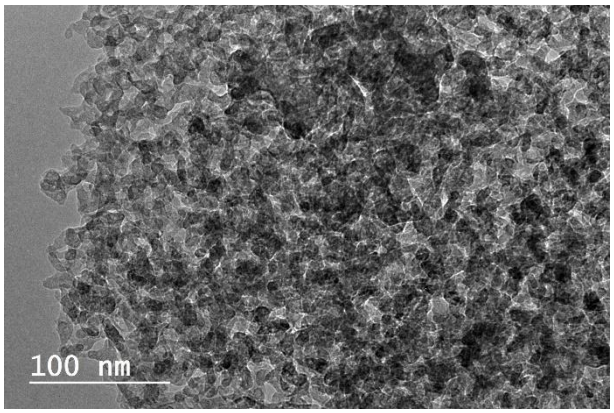


**Figure 3:** TEM image of F-$Al_2O_3$ before treatment under HF gas.

After surfactant extraction by ethanol Soxhlet, the peaks at 2 θ = 17.3, 20.0, 28.3, 34.9, 40.4, 53.3 and 58.5° (Fig. 4) observed on the XRD pattern of F-$Al_2O_3$. suggest the formation of either $(NH_4)_3AlF_6$ (ICDD 04-026-7606) or $AlF_3(H_2O)_6$ (ICDD 01-086-6306). As these two compounds are isostructural, it is not possible to differentiate them by this technique.

However, as the crystallization of $AlF_3(H_2O)_6$ requires peculiar methods such as the ionothermal synthesis [15], we can assume that the reflections lines observed on the X-ray pattern of the extracted F-$Al_2O_3$ rather correspond to $(NH_4)_3AlF_6$. The latter can be formed either during the initial step of the synthesis procedure or during the treatment under $NH_3$ atmosphere. The XRD pattern also shows the presence of an amorphous phase, characterized by a halo centered at around 2θ = 40°. After calcination at 500°C the fluorinated alumina is mainly amorphous, only traces of β-$AlF_3$ (ICDD 01-084-1672) are observed on the X-ray pattern (Fig. 4).

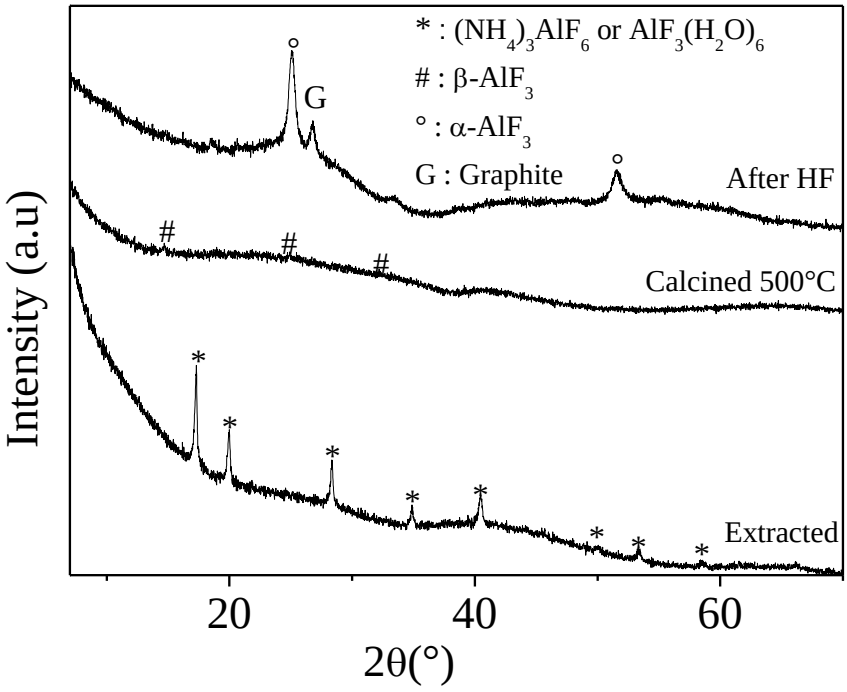


**Figure 4:** XRD pattern of F-$Al_2O_3$.

Therefore, the crystalline compound observed after extraction has been decomposed during this step. Indeed, in literature it is reported that β-$AlF_3$ can be obtained by thermal treatment of $(NH_4)_3AlF_6$ [16] and that $(NH_4)_3AlF_6$ is completely decomposed into $AlF_3$ at around 260°C [17]. After treatment under HF gas the appearance of the reflections at 2θ = 25.1 and 51.6° (Fig. 4), indicate that the crystallization of α-$AlF_3$ has begun (ICDD 01-080-1007), likely because of the further fluorination of the aluminium hydroxyfluoride. However, their intensities suggest that α-$AlF_3$ and β-$AlF_3$ are not well crystallized and that amorphous phase is still present. This can explain the stability of the structural parameters (specific surface area, pore volume) during the treatment under HF gas. The presence of graphite is due to graphite residue used to dilute the catalyst in the reactor in order to be in a differential regime.
The fluorine content, determined by X-ray fluorescence in the calcined F-$Al_2O_3$ is 13.5 wt.%.

### 3.2. Environment of aluminum and fluoride atoms of F-$Al_2O_3$.

The environments of F and Al have been probed by $^{27}Al$ (Fig. 5A) and $^{19}F$ NMR (Fig. 5B) analyses, respectively. Resonances have been attributed according to literature [18-22]. After calcination at 500°C and before treatment under HF gas, the $^{27}Al$ spectrum of F-$Al_2O_3$ exhibits signals at 59.5, 30.3, 2.2, -13.4 and -42.9 ppm (Fig. 5Aa). The resonance in the range of 50-60 ppm is assigned to aluminum atoms, which are tetrahedrally coordinated to the framework. A chemical shift at around 0 ppm (2.2 ppm here) is usually due to octahedrally coordinated Al [$AlO_6$]. The signal at 30.3 ppm correspond to Al in a pentahedral environment and could be due to $AlF_xO_{5-x}$ species. The presence of six-coordinated Al in aluminum fluoride is characterize by the chemical shift at -13.4 ppm [$AlF_6$]. The latter can also be an indication of Al in a mixed O and F environment [$Al(O_3F_3)$].
Finally the shoulder at about-42.9 ppm is attributed to $Al(O_nF_{6-n})$ species in partially hydrated $AlF_3.nH_2O$ ($n \leq 3$). After deconvolution resonances at -136.1, -140.9 , -173.5

and -184.9 ppm are detected on the $^{19}F$ spectrum (Fig. 5Ba). The two first ones characterize aluminium oxyfluoride environments $[AlO_{6-x}F_x]$ with x comprises between 1 and 6. More precisely, the signal at -136.1ppm comes from $[AlO_{6-x}F_x]$ unit where oxygen predominate with a trace amount of fluorine. The signal at -140.9 ppm corresponds to x value equal to 2 or 3. A resonance at -184.9 ppm is also observed belonging to terminally bound fluorine atoms to a single aluminium site. The signal at -173.5 ppm can be assigned to $AlF_6$, $AlF_3.nH_2O$ ($n \leq 3$). After the treatment under HF gas, the $^{27}Al$ resonances of $Al_2O_3$ disappear. Only two signals at -16.8 and -23.5ppm are still detected on the $^{27}Al$ spectrum (Fig. 5Ab). The first one is in accordance with aluminium in an octahedral environment $AlF_6$. The shoulder is related to the partially hydrated $AlF_3.nH_2O$ ($n \leq 3$). The $AlF_6$ environments is also evidenced by the presence of its typical resonance at –172.2 ppm on the $^{19}F$ NMR spectrum (Fig. 5Bb). Since no signal assigned to aluminium oxyfluoride environments is detected on the $^{27}Al$ spectrum, the second component at -163.9 ppm can be attributed to amorphous $AlF_3$ [23]. From the NMR results we can conclude that after synthesis aluminium oxyfluoride are formed. After treatment under HF gas a second fluorination step leads to the complete fluorination of $Al_2O_3$ to give $AlF_3$. In contrary to what is usually observed, this further fluorination under HF gas occurs without the modification of the specific surface area (Tables 1 and 2).

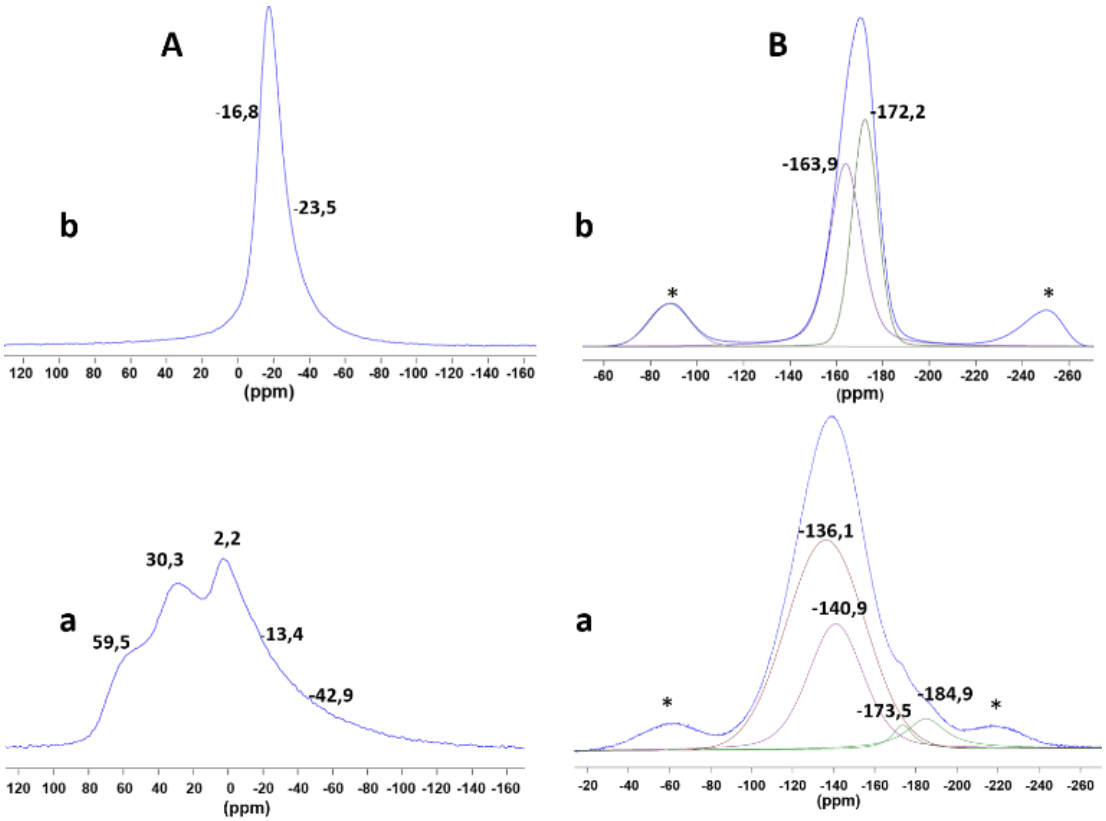


**Figure 5:** $^{27}Al$ (A) and $^{19}F$ spectra (B) of F-$Al_2O_3$ after calcination at 500°C (a) and calcination at 500°C followed by treatment under HF gas (b). *: spinning side bands.

### 3.3 Acidic properties of F-$Al_2O_3$.

Pyridine has been used as probe molecule to characterize by FTIR the number and the strength of the acidity the active sites (coordinatively unsaturated sites from magnesium or aluminum). As it can be seen from Table 3, the pure alumina has only Lewis sites (0.6 µmol.$m^{-2}$). The surface hydroxyl groups of $Al_2O_3$ are not sufficiently strong as Brønsted acid sites to protonate pyridine. By contrast the partially fluorinated alumina presents both Brønsted and Lewis acidity but the Lewis acid sites dominate (0.9 µmol.$m^{-2}$ against 0.2 µmol.$m^{-2}$). According to literature [18, 24], the Lewis sites are linked to the coordinatively unsaturated aluminum (CUSs) or defect sites at the surface. The Brønsted ones arise both from the formation of Al–F bonds at the surface and the presence of a proton rich atmosphere [25]. Comparing $Al_2O_3$ and F-$Al_2O_3$, the number of Lewis acid sites decreases from 184 to 110 µmol.$g^{-1}$, this can be due to the increase in the average coordination number of aluminum on the surface as fluorine replaces oxygen. However, in contrary to what it is reported in literature[13] here their concentration is increased from 0.6 to 0.9 µmol.$m^{-2}$. This is due to the surface effect. Except a slight increase of the Brønsted sites, the further treatment under HF gas does not modify the proportion of the acid sites. The persistence of the Brønsted acidity is in accordance with the detection of the partially hydrated $AlF_3.nH_2O$ ($n \leq 3$) observed on the $^{19}$FNMR spectra.

**Table 3**: Lewis and Brønsted acidity measurement by FTIR pyridine

| | $Al_2O_3$ | F-$Al_2O_3$ before treatment | F-$Al_2O_3$ after treatment |
|---|---|---|---|
| Lewis (µmol.$g^{-1}$) | 184 | 110 | 111 |
| Lewis (µmol.$m^{-2}$) | 0.6 | 0.9 | 1.0 |
| Brønsted (µmol.$g^{-1}$) | 0.0 | 29 | 39 |
| Brønsted (µmol.$m^{-2}$) | 0.0 | 0.2 | 0.4 |

### 3.4. Transformation of 2-chloropyridine under HF gas using of F-$Al_2O_3$ as support.

The obtained F-$Al_2O_3$ has been then impregnated by Mg and the performances measured for the transformation of 2-chloropyridine. As shown in Table 4, even if the quantity of active phase is much lower than bulk $MgF_2$ synthesized by the solvothermal method, fluorinated alumina-based catalysts present an activity per gram in the same range of order than this catalyst and an activity in mmol.$h^{-1}$.$g^{-1}$ three times higher than that obtained using commercial $AlF_3$ as support. In addition, they also have an excellent catalytic activity per magnesium atom, indicating a better accessibility of the catalytic sites. Indeed, what is very interesting is that its activity per magnesium atom is 16.5 times higher than that of the bulk $MgF_2$ and 3 times higher than the one of the supported catalyst obtained by using $AlF_3$ support prepared by other method. Since both supports lead to catalyst with similar activity per m² (0.4 mmol.$h^{-1}$.$m^{-2}$), the difference activity per Mg atom can be unambiguously relied to the surface effect.

**Table 4**: Transformation of 2-chloropyridine (T=350°C, 4h30, HF/$N_2$/2-ClPy=6/1.7/1). Effect of the support.

| Catalyst | Bulk $MgF_2$[1] | Mg2%wt./ $AlF_3$[2] | Mg2%wt./ F-$Al_2O_3$ |
|---|---|---|---|
| Activity (mmol.$h^{-1}$.$g^{-1}$) | 37 (±2) | 11 (±1) | 33(±2) |
| Activity (mmol.$h^{-1}$.$m^{-2}$) | 0.8 | 0.4 | 0.4 |
| Activity (x$10^{-21}$ mmol.$h^{-1}$.atom of $Mg^{-1}$) | 4 | 22 | 66 |

*[1]: prepared by hydro solvothermal method assisted by microwave heating using magnesium carbonate as precursor; [2] : commercial support*

This result clearly outlines the importance of dispersing the active phase on support with high specific surface area and having a high stability under the operating conditions. It should also be noted that operating conditions, in particular the amount of active phase, have not been optimized yet for the partially fluorinated alumina.

## 4. Conclusion

In summary, the dispersion of the active phase on mainly amorphous aluminum hydroxyfluoride with enhanced textural and acid properties leads to a new generation of efficient catalysts for the transformation of 2-chloropyridine under HF gas. These results demonstrate the potential of our synthetic method to obtain stable partially fluorinated alumina, which can contribute to the development of catalysts that are less « consuming » of atoms because they have a higher activity per atom. However, before considering the use of this material for catalytic reactions in an aqueous medium or for reactions generating water, its water tolerance should be investigated in detail. However, according to studies carried out on non-fluorinated alumina [13], we can expect good tolerance to water at room temperature. Indeed, On the basis of SAXS, XRD and $N_2$ adsorption-desorption analyses, we have shown that when treated into boiling water or exposed to water vapor the alteration of the mesostructure occurs quickly. Its collapse has been attributed to the crystallization of the amorphous alumina walls into aluminum hydroxides, mainly boehmite, upon the hydration of the alumina. By contrast at room temperature when placed in water at room temperature, the mesostructured is observed after 48 hours of immersion but the specific surface area drops from 365 $m^2/g$ to 264 $m^2/g$. This phenomenon has been attributed to the formation of small boehmite particles due to the hydration of the surface [13].

## Credit authorship contribution statement

Jean-Luc Blin: Writing - original draft, Supervision, Conceptualization; Julien Dieu: Investigation; Bénédicte Lebeau: Writing - original draft, Supervision, Conceptualization; Laure Michelin: Investigation; Séverinne Rigolet: Investigation; Sylvette Brunet: Writing - original draft, Supervision, Conceptualization.

## Acknowledgements

We would like to thank the platforms « X-ray Diffraction, Electronic Microscopy, NMR » of IS2M, especially Loïc Vidal is warmful thanked for the TEM observations.

## Conflicts of interest

The authors declare that they have no competing interests

## Funding

This research received no external funding.

**References**


[1] J. Wang, M. Sánchez-Roselló, J. L. Aceña, C. Del Pozo, A. E. Sorochinsky, S. Fustero, V. A. Soloshonok, H. Liu, *Chem. Rev.* **2017**, *114*, 2432.

[2] C. Pfleger, P. Waldmier, S. Wang, US 2008/0221327 A1, 2008.

[3] N. Yoneda, T. Fukuhara, *Tetrahedron* 1996, *52*, 23.

[4] G. Fujioka (The Dow Chemical Company), US Pat. 4,680,406, 1986

[5] A. Astruc, C. Cochon, S. Dessources, S. Célérier, S. Brunet, *Appl. Catal. A Gen.* **2013**, *453*, 20.

[6] A. Astruc, S. Célérier, E. Pavon, A.S Mamede, L. Delevoye, S. Brunet, *Appl. Catal. B Environ.* 2017, *204*, 107.

[7] Z. Goharibajestani, Y. Wang, V. Camus-Génot, S. Arrii, J.D. Comparot, B. Polteau, J. Lhoste, C. Galven, V. Gunes, A. Hémon-Ribaud, S. Pascual, M. Body, C. Legein, V. Maisonneuve, S. Brunet, A. Guiet, *ACS Appl. Nano Mater.***2021**, *4*, 10601.

[8] A. Loustaunau, R. Fayolle-Romelaer, S. Celerier, A. D'Huysser, L. Gengembre, S. Brunet, *Catal. Lett.* **2010**, *138*, 215.

[9] E. Kemnitz, U. Groß, S. Rüdiger, C. S. Shekar, *Angew. Chem. Int. Ed.* **2003**, *42*, 4251.

[10] H. Pines, W. Haag, *J. Am. Chem. Soc*. **1960**, *82*, 2471.

[11] G. Busca, *Adv. Catal.* **2014**, *57*, 319.

[12] T. Skapin, *J. Mater. Chem.* **1995**, *5*, 1215.

[13] J.L. Blin, F. Jonas, L. Michelin, S. Rigolet, L. Josien, L. Vidal, L. Richaudeau, B. Lebeau, *Microporous Mesoporous Mater.* **2024**, *367*, 112997.

[14] D.Massiot, F.Fayon, M.Capron, I.King, S.Le Calvé, B.Alonso, J-O.Durand, B.Bujoli, Z.Gan, G.Hoatson, Magn. Reson. Chem. 2002, 40, 70

[15] G. Wang, A.V. Mudring, *Solid State Sci.* **2016**, *61*, 58.

[16] L Francke, E. Durand, A. Demourgues, A. Vimont,M. Daturi, A. Tressaud, *J. Mater. Chem.* **2003**, *13*, 2330.

[17] X.W. Hu, L. Li, B.L. Gao, Z.N. Shi, H. Li, J.J. Liu, Z.W. Wang, *Trans. Nonferrous Met. Soc. China* **2011**, *21*, 2087.

[18] P.J. Chupas, C.P. Grey, *J. Catal.* **2004**, *224*, 69.

[19] W. Zhang, M. Sun, R. Prins, *J. Phys. Chem. B* **2002**, *106*, 11805.

[20] L. Fischer, V. Harle, S. Kastelan, J.B. d'Espinose de la Caillerie, *Solid State NMR* **2000**, *16*, 85.

[21] R. König, G. Scholz, A. Pawlik, C. Jäger, B. van Rossum, H. Oschkinat, E. Kemnitz, *J. Phys. Chem. C* **2008**, *112*, 15708.

[22] C.P. Marshall, G. Scholz, T. Braun, E. Kemnitz, *Catal. Sci. Technol.* **2020**, *10*, 391.

[23] P.J. Chupas, D.R. Corbin, V. N. M. Rao, J.C. Hanson, C.P. Grey, *J. Phys. Chem. B* **2003**, *107*, 8327.

[24] L. Ahrem, J. Wolf, G. Scholz, E. Kemnitz, *Catal. Sci. Technol.* **2018**, *8*, 1404.

[25] D. Dambournet, A. Demourgues, C. Martineau, J. Majimel, M. Feist, C. Legein, J.Y. Buzaré, F. Fayon, A. Tressaud, *J. Phys. Chem. C* **2008**, *112*, 12374.